Reversible Solvent Vapor-Mediated Phase Changes in Nanocrystal Superlattices

Brian W. Goodfellow and Brian A. Korgel*

Department of Chemical Engineering, Texas Materials Institute, Center for Nano and Molecular Science and Technology, The University of Texas at Austin, Austin, Texas 78712-1062, United States

ABSTRACT Colloidal nanocrystals are being explored for use in a variety of applications, from solar cells to transistors to medical diagnostics and therapy. Ordered assemblies of nanocrystals, or superlattices, are one particularly interesting class of these materials, in which the nanocrystals serve as modular building blocks to construct nanostructures by self-assembly with spatial and temporal complexity and unique properties. From a fundamental perspective, the nanocrystals are simple molecular models that can be manipulated and studied to test statistical mechanical and thermodynamic models of crystallization and disorder. An article by Bian *et al.* in this issue of *ACS Nano* reports surprising new phase behavior in semiconductor nanocrystal superlattices: *reversible* transitions between non-close-packed body-centered cubic (bcc) and body-centered tetragonal (bct) structures, and close-packed face-centered cubic (fcc) structures, observed by real-time *in situ* grazing incidence small-angle X-ray scattering (GISAXS) measurements, upon solvent vapor exposure and increased interparticle separation. These studies offer new insight and raise new questions about superlattice structure and the forces that control self-assembly. Accompanying computer simulations show that ligand–ligand interactions are important. Furthermore, it appears that ligand-coated nanocrystals have more in common with soft microphase-separated materials, like diblock copolymers and surfactant assemblies, than previously realized.

Living systems are well-known to organize by self-assembly with complexity on multiple length and time scales.[1] Many natural *nonliving* materials also exhibit sophisticated organization by self-assembly. The opal is a good example of this, composed of highly monodisperse collections of submicrometer silica particles molded over time and packed tightly into a lattice. As synthetic methods for nanocrystals of a wide range of materials have developed—along with an understanding of their unique properties—nanocrystal self-assembly has been targeted as a route to obtain materials with complicated structure and unprecedented function.[2−4] The concept is simple: combine nanocrystals and allow (or coax) them to self-assemble into ordered superstructures. One strategy is to merge synthetic nanocrystals and molecules with biological self-assembly motifs.[5,6] To accomplish this, a fundamental understanding of the forces and processes that control self-assembly is needed. As Bian *et al.*[7] show in this issue of *ACS Nano*, even an assemblage of monodisperse nanocrystals—the simplest system possible—is still offering up new surprises.

On the basis of simple packing rules of spheres, a monodisperse collection of spherical, organic ligand-coated nanocrystals is expected to form a face-centered cubic (fcc) lattice. When dispersed in a good solvent, the nanocrystals experience a short-ranged steric repulsion, similar to that of hard spheres.[8] When the nanocrystals are compressed together and the density of the collection exceeds a critical value—for example, when the solvent is evaporated from the dispersion—the nanocrystals spontaneously order into a superlattice. This ordering transition is driven by entropy. With negligible energetic interactions between nanocrystals, only the excluded volume of each particle matters and the structure with the highest entropy is favored. It is easy to appreciate that the fcc lattice is the structure with the highest packing entropy by considering the entropy of an ideal gas of N particles in a volume V: $S/N = k \ln V$ (k is Boltzmann's constant). The *free volume entropy* depends on the way the particles are arranged. For a collection of hard spheres of volume v_s, the free volume is $V - Nv_s = 1 - (\phi/\phi_c)$, expressed in terms of the volume fraction of particles ϕ, and the jamming limit or maximum density of the spheres ϕ_c, determined by the specific structural arrangement, and the free volume entropy is $S/N \propto k \ln(1 - (\phi/\phi_c))$. A disordered collection of spheres can only pack to a limit of $\phi_c = 64\%$ before becoming *jammed*. Spheres in an fcc lattice—the densest possible arrangement of spheres—can achieve much higher densities, up to $\phi_c = 74\%$. It is obvious then that the free volume entropy of particles at a density of 64% is much higher when arranged in an fcc lattice than in a jammed configuration (where $S = 0$).

* Address correspondence to korgel@che.utexas.edu.

Published online April 26, 2011
10.1021/nn201273c

Indeed, fcc superlattices of a wide variety of nanocrystals have been observed.[2,3,8,12]

However, when the solvent has evaporated, the nanocrystals are clearly not interacting as hard spheres. The nanocrystals in a "dry" superlattice are held together by strong cohesive interactions between neighboring ligands and nanocrystals. The melting point of dodecanethiol, for example, is about −8 °C, but a superlattice of dodecanethiol-capped gold nanocrystals is a solid at room temperature. Perhaps not surprisingly then, a variety of superlattice structures in addition to fcc have been observed, including hexagonal close-packed (hcp),[9,10] body-centered cubic (bcc),[3,11,12] body-centered tetragonal (bct),[3,12] and the simple hexagonal (sh)[10] lattice. The bcc, bct, and sh lattices are particularly interesting because they are not close-packed structures and the free volume, or packing, entropy of the spheres is not maximized. For example, ϕ_c = 68% for a bcc lattice. The situation has become ever more complicated with the study of ordered arrangements of nanocrystals of two different sizes, so-called binary nanocrystal superlattices. By 2006, a tremendous structural diversity of binary nanocrystal superlattices had been observed, many of which do not follow simple space-filling rules expected for hard spheres.[4]

Nonetheless, most superlattices, even binary nanocrystal superlattices,[13−15] do not deviate all that far from expectations based on maximized sphere packing density, and this concept has served as an acceptable conceptual guideline for understanding superlattice structure. The challenge has been to understand how the ligand shell contributes to superlattice order. Unlike submicrometer colloidal particles, such as those that form opals in nature, ligand-coated nanocrystals have a significant volume of deformable soft organic shell material, making them "soft spheres" with an inner rigid, nondeformable core.[8] The fcc lattice is favored over bcc (and bct) on the basis of both cohesive energy (simply summing up the pairwise attractions between neighboring particles: 12 and 8 nearest neighbors for fcc and bcc, respectively) and free volume entropy. So, the question is: Why would bcc superlattices form instead of fcc superlattices?

In previous independent studies of alkanethiol-capped gold[3] and silver[12] nanocrystals, fcc superlattices were observed when the ligand layers were relatively thin compared to the inorganic core size, and bcc superlattices were observed when the ligand layer was relatively thick. The superlattice structure could be charted as a function of the ratio of average ligand length $\langle L \rangle$, to inorganic core radius R. A critical value of $\langle L \rangle / R$ between 0.6 and 0.7 was observed for both alkanethiol-capped gold and silver nanocrystals.[3,12] Considering that the ligands effectively augment repulsion between the inorganic cores of the nanocrystals by screening their van der Waals attractions, increased $\langle L \rangle$ (relative to R) indicates that the repulsion becomes longer-ranged for high $\langle L \rangle / R$, apparently favoring the more open bcc lattice over the denser fcc lattice.[12] Charge-stabilized colloids[16] and block copolymer micelles[17] both undergo qualitatively similar transitions from fcc to bcc when the range of repulsive interactions becomes more extended. For example, charge-stabilized colloids form fcc lattices when the repulsion between charged particles is highly screened with an interaction potential similar to hard spheres and form bcc lattices when the screening is low and the interaction potential is strongly repulsive and long-ranged. The free volume entropy always favors fcc order; however, when the repulsion between particles is strong, there is an energetic contribution to the lattice energy that favors a more open, less dense structure. The bcc lattice is, in fact, the most stable structure for an idealized dense collection of point charges.[18] Polymer micelles have qualitatively similar structure to ligand-coated nanocrystals, with a largely nondeformable core surrounded by a soft corona. "Crew-cut" polymer micelles with a thin corona layer and a short-ranged weak repulsion between micelles tend to order into fcc lattices, whereas "hairy" micelles with more extended coronas and longer-ranged repulsion form bcc lattices.[17] This type of soft sphere model explained at least semiquantitatively the formation of the non-close-packed bcc (and related bct) superlattices.[3,12]

An Updated Model of bcc−fcc Superlattice Transition. A new study reported by Bian *et al.*[7] in this issue of *ACS Nano* squarely challenges this model. They performed grazing incidence small-angle X-ray scattering (GISAXS) measurements on oleic-acid-capped PbS and PbSe nanocrystals and observed that the nanocrystals tended to form bcc and bct superlattices. (Note that the bct lattice is quite similar to the bcc lattice, but with a lattice distortion in the *c*-direction.) On the basis of past observations of bcc and bct alkanethiol-coated gold and silver nanocrystals, the PbS and PbSe nanocrystals should then have a relatively large $\langle L \rangle / R$ ratio, higher than 0.6−0.7.[3,12] This was not the case. The values of $\langle L \rangle / R$ of the PbS and PbSe nanocrystals were lower than expected, ranging between only 0.5 and 0.6. Why then were the nanocrystals not forming fcc superlattices?

Perhaps the value of $\langle L \rangle / R$ for an fcc−bcc transition depends on the details of the system. For example, block copolymer micelles have a much larger critical value of $\langle L \rangle / R$, near 1.5, for the fcc−bcc transition. Furthermore, the value of 0.6−0.7 based on alkanethiol-coated gold and silver nanocrystals may not apply quantitatively to oleic-acid-capped PbS or PbSe nanocrystals. Oleic acid is itself a rather long C_{18} capping ligand with a double bond, compared to the typical alkanethiol chains less than C_{12} studied for Au and Ag. Also, PbS and PbSe nanocrystals have been observed in some cases to have charged surfaces that could certainly influence

the interparticle potential.[10] In their study, Bian *et al.*[7] carried out a decisive solvent vapor-annealing experiment that clearly showed something was missing from the simple consideration of $\langle L \rangle / R$ as a structure-determining parameter. While conducting *in situ* GISAXS to observe superlattice structure directly, they found that their bcc and bct superlattices transformed to fcc when the superlattice *expanded*, in other words when $\langle L \rangle / R$ increased—running *counter* to the simple guidelines that fcc superlattices are favored at small $\langle L \rangle / R$ and bcc favored at larger $\langle L \rangle / R$.

As Bian *et al.* showed, the structural transitions from bcc to fcc are completely reversible and would not be detected by *ex situ* analysis after the removal of the solvent vapor.

Solvent vapor annealing is well-known to lead to dramatic structural changes in films of diblock copolymers[19] but has not been extensively studied in the case of nanocrystal superlattices. To detect the structural changes during solvent vapor annealing, GISAXS, or some probe of superlattice structure, must be carried out simultaneously. As Bian *et al.*[7] showed, the structural transitions are completely reversible and would not be detected by *ex situ* analysis after the removal of the solvent vapor. Therefore, electron microscopy—the workhorse analytical tool for the nanomaterials field—is not well-suited for these kinds of studies. Bian *et al.* exposed their bcc (and bct) oleic-acid-coated PbS and PbSe superlattices to octane vapor and the superlattice transformed to fcc (see Figure 1). Octane is a good solvent for the ligands and swelled the superlattice, increasing the interparticle separation. Higher levels of solvent exposure disordered the lattice. The structural transitions were completely reversible, with the superlattice reverting back to its original structure after removal of the solvent vapor. In comparison to transmission SAXS measurements, GISAXS provides additional information about the orientation of the superlattice with respect to the substrate, as well as very high sensitivity for probing thin films (including monolayers) of nanocrystals. GISAXS showed that the solvent vapor expanded the superlattice significantly, and multiple higher-order diffraction spots were observed in the experiments, confirming unambiguously the superlattice structures of fcc, bcc, and bct. Under some conditions, the rate of solvent removal could influence the superlattice structure, but it was clear from their study that using $\langle L \rangle / R$ as a simple structure-determining parameter is flawed.

Bian *et al.*[7] also observed that nanocrystals in the bcc and bct superlattices exhibited a high degree of crystallographic registry or orientational order between particles. Simultaneous grazing incidence wide-angle X-ray scattering (GIWAXS) exhibited lobes, indicating that the PbS and PbSe crystal planes in the nanocrystal cores were aligned throughout the superlattice (see Figure 1 of ref 7). On the other hand, the fcc superlattices showed no such preferential crystallographic orientation. Detailed computer simulations of the ligand–ligand interactions between neighboring nanocrystals were carried out, and the ligand coverage surrounding each nanocrystal was observed to be sensitive to the particular crystal facet exposed on the nanocrystal surface. Simulations of interacting nanocrystals indicated that this anisotropic ligand coverage can give rise to interparticle interactions that depend rather strongly on the relative orientations of the crystal lattice within the core of the neighboring nanocrystals. A qualitatively similar model was proposed by Harfenist *et al.*[20] in 1996 to account for crystallographic registry between alkanethiol-capped Ag nanocrystals observed in fcc superlattices. The models of Harfenist *et al.* and Bian *et al.* for Ag and PbSe (and PbS) nanocrystals both propose a truncated octahedral shape for the nanocrystals with exposed (100) and (111) surface facets and preferential ligand–ligand interactions deriving from the (111) facets. In the case of the Ag nanocrystals, this was believed to be the driving force for fcc superlattice structure, whereas Bian *et al.* propose that the preferential ligand–ligand interactions between (111) facets on neighboring nanocrystals help stabilize the bcc (and bct) structure of the PbS and PbSe superlattices, essentially then fitting into the bcc Wigner–Seitz cell (illustrated in Figure 1B). Others have also proposed that ligand–ligand interactions may be important and potentially structure determining. Luedtke and Landman[21] computed ligand–ligand interactions between alkanethiol-coated Au nanocrystals and proposed them to be responsible for bcc and bct superlattice structures. Recent experimental work on oleic-acid-capped PbSe nanocrystals by Wang *et al.*[22] also appears to indicate that ligand–ligand interactions can be important and structure determining.

Bian *et al.*[7] clearly show that there is more to the story of the bcc–fcc superlattice transition than increased $\langle L \rangle / R$ favoring the formation of more open, non-close-packed superlattice structure. Indeed, increasingly sophisticated computer simulations are showing that ligand–ligand interactions play an important role in superlattice structure. However, it is worth discussing whether microscopic interactions between ligands on neighboring nanocrystals, which may be very specific for particular nanocrystal/capping ligand combinations, are *critical* to understanding nanocrystal superlattice structure. After all, the prevalent fcc superlattice structure observed for many different nanocrystals is consistent with expectations based on free volume entropy and

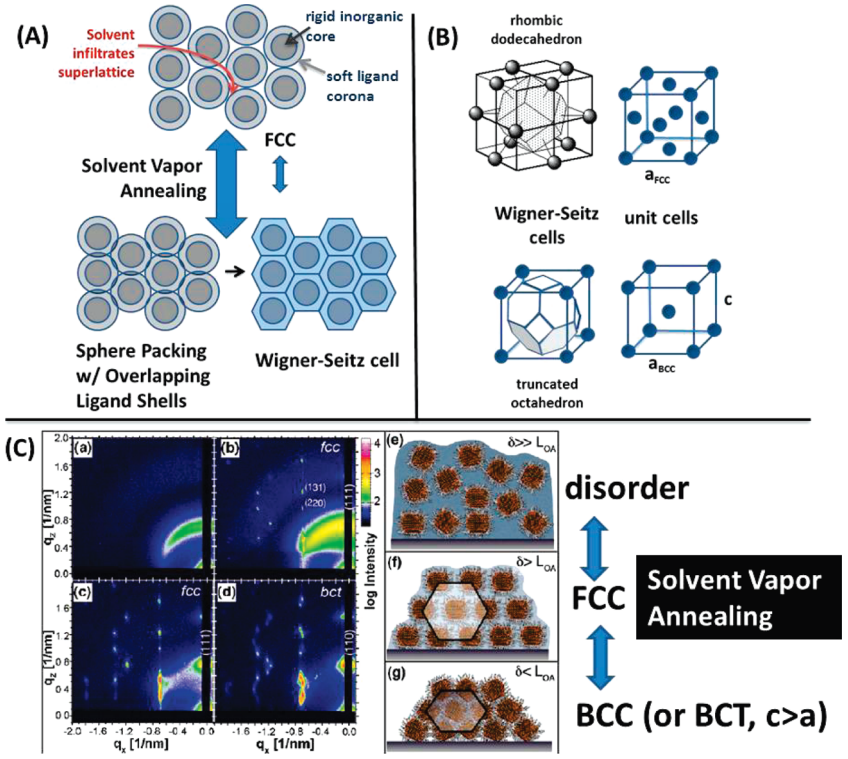

Figure 1. (A) Illustration of how ligand packing frustration leads to a change in superlattice symmetry from fcc to bcc. When the ligands are more extended, as is the case with solvent vapor exposure, there is little ligand deformation around the nanocrystals and the free volume entropy favors fcc packing of the nanocrystals. In the denser arrangement of nanocrystals, however, the ligands must conform more strongly to the polyhedral Wigner–Seitz cell of the lattice. The Wigner–Seitz cell is more spherical in the bcc unit cell than in the fcc unit cell, as illustrated in (B). Therefore, the ligands are more uniformly spread in the bcc superlattice than in the fcc superlattice. (C) Solvent vapor-annealing data from Bian *et al.*[7] GISAXS of oleic-acid-capped PbS nanocrystals. The dry superlattice forms a bct structure. Solvent annealing leads to an increase in interparticle separation, as shown in the schematic, and a change in superlattice structure to fcc. Increased solvent exposure further separates the nanocrystals and the superlattice disorders. The structural transitions are reversible. Panel (C) is adapted from ref 7. Copyright 2011 American Chemical Society.

(somewhat attractive) isotropic interparticle interactions, and in many cases, the soft deformable ligand shell simply fills interstitial space in the superlattice as needed, like glue. We would also like to point out that the solvent annealing result of a transition from bcc to fcc with increased interparticle separation is, in fact, consistent with expectations for a collection of soft sphere particles, even though seemingly inconsistent with expectations based on the alkanethiol-capped Au[3] and Ag[12] nanocrystals.

As Bian *et al.*[7] found, and is illustrated in Figure 1, the superlattice expanded when the solvent molecules penetrated the intervening ligands. This should reduce the interparticle attractions significantly,[8,12] and thus, one explanation for the observed bcc–fcc transition is that solvent vapor annealing actually drives the nanocrystals closer toward the situation of a collection of hard sphere nanocrystals. The spreading out of the nanocrystals decreases the amount of ligand deformation, as well, as illustrated in Figure 1A. Under these conditions, the free volume entropy of the fcc lattice becomes important and leads to a transformation of the superlattice from bcc to fcc. Indeed, further solvent annealing disordered the superlattice—the equivalent of melting. Such a progression from bcc to fcc to disorder has been predicted for soft Hertzian spheres, or particles separated by a flexible spring-like layer with a temperature-dependent spring constant.[23] As the temperature increases, the lattice expands and the particles behave as densely packed spheres with only weak energetic interactions. Here, the solvent plays the role of temperature, stretching the ligands and reducing the interparticle interactions. Weak interparticle interactions more closely approximate hard spheres and free volume entropy takes over, driving the particles into an fcc lattice.

> Bian *et al.* clearly show that there is more to the story of the bcc–fcc superlattice transition than increased $\langle L \rangle / R$ favoring the formation of more open, non-close-packed superlattice structure.

So, why do the nanocrystals order into the bcc (or closely related bct) lattice when the solvent evaporates? Whereas the fcc lattice is special

in that it is the densest possible collection of spheres, the bcc lattice is special in that, of all possible arrangements, it is the arrangement that minimizes interfacial area between neighboring spheres.[24] The fact that this is the case can be deduced by examining and comparing the Wigner–Seitz cells of bcc and fcc lattices (at least that the interfacial contact area in a bcc lattice is less than in an fcc lattice) (Figure 1). The Wigner–Seitz cells are Voronoi tessellations, or space-filling polyhedra that represent the shape of the boundary between each "particle" needed to completely fill the volume. (A sphere has the lowest surface area to volume ratio of any shape but cannot fill space completely when packed together; the polyhedra fill the space completely when packed together.) The truncated octahedral Wigner–Seitz cell of the bcc lattice is more spherical than the rhombic dodecahedron of the fcc lattice, thus better minimizing the interfacial area between neighbors in the lattice.[24] To see why this matters, consider how the ligand must deform, as in the case of the PbS and PbSe nanocrystals, as the solvent evaporates from the superlattice and the interparticle separation decreases. As shown in Figure 1, when the superlattice shrinks and the nanocrystals are pressed together, the ligands can no longer spread uniformly around the nanocrystals and are forced to spread into the interstitial space of the lattice. The ligand shell can no longer take on a roughly spherical shape (as desired by the ligands) but must conform to the shape of a "faceted" space-filling polyhedron of the superlattice. This same phenomena occurs in sphere-forming block copolymers and is referred to as chain-packing frustration.[25] Chain-packing frustration has a significant impact on diblock copolymer assembly and is the reason that sphere-forming diblock copolymer melts only form bcc lattices and never fcc lattices—the extent of packing frustration is significantly lower in the bcc lattice than in the fcc lattice.[26] (Incidentally, only when loaded with solvent and transformed to a dense collection of micelles do diblock copolymers form fcc lattices, in many ways analogous to the PbS and PbSe nanocrystals studied by Bian *et al.*) Perhaps the reason that ligand-coated nanocrystals form bcc superlattices is that, even though free volume entropy favors fcc packing of the spheres, the frustrated ligand packing pushes the structure into a bcc lattice with its more spherically symmetric Wigner–Seitz cell. The role of ligand-packing frustration has also been considered by Chen *et al.*[13,14] in binary nanocrystal superlattice assembly, but they ruled it out. On the basis of the prevalence of bcc superlattices of ligand-coated nanocrystals that have now been observed, it appears to us that ligand-packing frustration is indeed important.

Perhaps the reason that ligand-coated nanocrystals form bcc superlattices is that, even though free volume entropy favors fcc packing of the spheres, the frustrated ligand packing pushes the structure into a bcc lattice with its more spherically symmetric Wigner–Seitz cell.

Perhaps an alternative way of looking at ligand-coated nanocrystal superlattices is to view them as microphase-separated (or really, *nano*phase-separated) materials of inorganic cores embedded in a sea of soft organic material. If the ligands were not bound to the nanocrystals, phase segregation would occur and the superlattice structure would be destroyed. In at least one instance, temperature-dependent SAXS from an alkanethiol-coated Ag nanocrystal superlattice has exhibited the expected signatures of a microphase-separated system.[27] Diblock copolymers with relatively simple chemical makeups have relatively complicated phase behavior, in large part due to ligand-packing frustration in combination with the free volume entropy and sphere-packing constraints of the spherical domains.[26]

The study by Bian *et al.*[7] has opened a new line of inquiry about nanocrystal superlattice self-assembly and perhaps a new way of thinking about them. For the first time, reversible structure changes have been demonstrated. This was enabled by the use of an added solvent instead of temperature, which has typically led to decomposition of the nanocrystals (*i.e.*, ligand desorption and vaporization) before any structural changes in the superlattice can occur.[3] With *in situ* GISAXS, it was possible to correlate the interparticle spacing directly with superlattice structure and, combined with GIWAXS, to correlate internal crystallographic registry between nanocrystals in the superlattice. Instead of thinking of these superlattices as collections of spherical particles, it is probably more accurate to consider them as spatially ordered microphase-separated materials that follow many of the same "rules" as diblock copolymers. This would imply that the fcc superlattice is really more of an exception and the bcc superlattice more of the rule. Furthermore, based on the fact that relatively simple diblock copolymers can exhibit complicated phase diagrams,[26] it is reasonable to believe that nanocrystals should also exhibit a relatively diverse range of structures. Of course, the main difference between diblock copolymers and nanocrystals is that, unlike in diblock copolymers, the radius of curvature for nanocrystals is fixed by the nanocrystal size. Furthermore, the nanocrystal core is inorganic and has particular crystallographic facets exposed. Bian *et al.* showed that this can also be important and lead to subtle deviations from isotropic interparticle potentials as well

as produce orientational correlations between nanocrystals in superlattices that would not have an analogy in diblock copolymers. For this reason alone, better microscopic models of the interactions between ligands and ligand-coated cores are needed. In the end, the conceptual model of nanocrystals as soft spheres ordered into lattices continues to have merit, but as more experimental data continue to be acquired, these concepts will continue to be refined and tested.

Acknowledgment. This work was supported in part by funding from the Robert A. Welch Foundation (F-1464) and the National Science Foundation (DMR-0807065).

REFERENCES AND NOTES

1. Stewart, I. *Life's Other Secret: The New Mathematics of the Living World*; Wiley: New York, 1998.
2. Murray, C. B.; Kagan, C. R.; Bawendi, M. G. Self-Organization of CdSe Nanocrystallites into Three-Dimensional Quantum Dot Superlattices. *Science* **1995,** *270*, 1336–1338.
3. Whetten, R. L.; Shafigullin, M. N.; Khoury, J. T.; Schaaff, T. G.; Vezmar, I.; Alvarez, M. M.; Wilkinson, A. Crystal Structures of Molecular Gold Nanocrystal Arrays. *Acc. Chem. Res.* **1999,** *32*, 397–406.
4. Shevchenko, E. V.; Talapin, D. V.; Kotov, N. A.; O'Brien, S.; Murray, C. B. Structural Diversity in Binary Nanoparticle Superlattices. *Nature* **2006,** *439*, 55–59.
5. Dylla, R. J.; Korgel, B. A. Temporal Organization of Nanocrystal Self-Assembly. *ChemPhysChem* **2001,** *2*, 62–64.
6. Alivisatos, A. P.; Johnsson, K. P.; Peng, X.; Wilson, T. E.; Loweth, C. J.; Bruchez, M. P.; Schultz, P. G. Organization of `Nanocrystal Molecules' Using DNA. *Nature* **1996,** *382*, 609–611.
7. Bian, K.; Choi, J. J.; Kaushik, A.; Clancy, P.; Smilgies, D.-M.; Hanrath, T. Shape-Anisotropy Driven Symmetry Transformations in Nanocrystal Superlattice Polymorphs. *ACS Nano* **2011**, 10.1021/nn103303q.
8. Korgel, B. A.; Fullam, S.; Connolly, S.; Fitzmaurice, D. Assembly and Self-Organization of Silver Nanocrystal Superlattices: Ordered "Soft Spheres". *J. Phys. Chem. B* **1998,** *102*, 8379–8388.
9. Harfenist, S. A.; Wang, Z. L.; Whetten, R. L.; Vezmar, I.; Alvarez, M. M. Three-Dimensional Hexagonal Close-Packed Superlattice of Passivated Ag Nanocrystals. *Adv. Mater.* **1997,** *9*, 817–822.
10. Talapin, D. V.; Shevchenko, E. V.; Murray, C. B.; Titov, A. V.; Král, P. Dipole–Dipole Interactions in Nanoparticle Superlattices. *Nano Lett.* **2007,** *7*, 1213–1219.
11. Whetten, R. L.; Khoury, J. T.; Alvarez, M. M.; Murthy, S.; Vezmar, I.; Wang, Z. L.; Stephens, P. W.; Cleveland, C. L.; Luedtke, W. D.; Landman, U. Nanocrystal Gold Molecules. *Adv. Mater.* **1996,** *8*, 428–433.
12. Korgel, B. A.; Fitzmaurice, D. Small-Angle X-ray Scattering Study of Silver-Nanocrystal Disorder-Order Phase Transitions. *Phys. Rev. B* **1999,** *59*, 14191–14201.
13. Chen, Z.; Moore, J.; Radtke, G.; Sirringhaus, H.; O'Brien, S. Binary Nanoparticle Superlattices in the Semiconductor–Semiconductor System: CdTe and CdSe. *J. Am. Chem. Soc.* **2007,** *129*, 15702–15709.
14. Chen, Z.; O'Brien, S. Structure Direction of II–VI Semiconductor Quantum Dot Binary Nanoparticle Superlattices by Tuning Radius Ratio. *ACS Nano* **2008,** *2*, 1219–1229.
15. Smith, D. K.; Goodfellow, B.; Smilgies, D.-M.; Korgel, B. A. Self-Assembled Simple Hexagonal AB_2 Binary Nanocrystal Superlattices: SEM, GISAXS, and Defects. *J. Am. Chem. Soc.* **2009,** *131*, 3281–3290.
16. Kremer, K.; Robbins, M. O.; Grest, G. S. Phase Diagram of Yukawa Systems: Model for Charge-Stabilized Colloids. *Phys. Rev. Lett.* **1986,** *57*, 2694–2697.
17. McConnell, G. A.; Gast, A. P. Predicting Disorder–Order Phase Transitions in Polymeric Micelles. *Phys. Rev. E* **1996,** *54*, 5447–5455.
18. Carr, W. J. Energy, Specific Heat, and Magnetic Properties of the Low-Density Electron Gas. *Phys. Rev.* **1961,** *122*, 1437–1446.
19. Albert, J. N. L.; Epps, T. H. Self-Assembly of Block Copolymer Films. *Mater. Today* **2010,** *13*, 24–33.
20. Harfenist, S. A.; Wang, Z. L.; Alvarez, M. M.; Vezmar, I.; Whetten, R. L. Highly Oriented Molecular Ag Nanocrystal Arrays. *J. Phys. Chem.* **1996,** *100*, 13904–13910.
21. Luedtke, W. D.; Landman, U. Structure, Dynamics, and Thermodynamics of Passivated Gold Nanocrystallites and Their Assemblies. *J. Phys. Chem.* **1996,** *100*, 13323–13329.
22. Wang, Y.; Dai, Q.; Wang, L.; Zou, B.; Cui, T.; Liu, B.; Yu, W. W.; Hu, M. Z.; Zou, G. Mutual Transformation between Random Nanoparticles and Their Superlattices: The Configuration of Capping Ligand Chains. *J. Phys. Chem. C* **2010,** *114*, 11425–11429.
23. Pàmies, J. C.; Cacciuto, A.; Frenkel, D. Phase Diagram of Hertzian Spheres. *J. Chem. Phys.* **2009,** *131*, 044514.
24. Ziherl, P.; Kamien, R. D. Maximizing Entropy by Minimizing Area: Towards a New Principle of Self-Organization. *J. Phys. Chem. B* **2001,** *105*, 10147–10158.
25. Grason, G. M. The Packing of Soft Materials: Molecular Asymmetry, Geometric Frustration and Optimal Lattices in Block Copolymer Melts. *Phys. Rep.* **2006,** *433*, 1–64.
26. Lee, S.; Bluemle, M. J.; Bates, F. S. Discovery of a Frank-Kasper's Phase in Sphere-Forming Block Copolymer Melts. *Science* **2010,** *330*, 349–353.
27. Korgel, B. A. Correlated Membrane Fluctuations in Nanocrystal Superlattices. *Phys. Rev. Lett.* **2001,** *86*, 127–130.